

Optimized Stretch Processing Compensation for FMCW Phase-Attached Radar-Communications

Cenk Sahin*, Patrick M. McCormick*, and Shannon D. Blunt†

*Sensors Directorate, Air Force Research Laboratory, Wright-Patterson Air Force Base, OH

†Department of Electrical Engineering & Computer Science, University of Kansas, Lawrence, KS

Abstract—The phase-attached radar-communications (PARC) framework facilitates the co-design of these different functions within a common frequency modulated (FM) waveform, thereby enabling the operation of both without sacrificing transmission resources (i.e. power, time, frequency) needed for the primary radar function. Recently, the original pulsed PARC structure was extended to an FM continuous wave (FMCW) arrangement that maximizes data throughput. The resulting FMCW PARC waveforms were successfully demonstrated in an open-air environment for a ground-based moving target indication (MTI) application using a recent form of stretch processing that compensates for deviations from the linear chirping reference signal.

However, the waveform-agile nature of PARC, which is necessary in order to convey information, does incur a performance cost that takes the form of range sidelobe modulation (RSM) of the clutter. To address this RSM degradation, here we introduce a range-dependent mismatched filtering approach for FMCW PARC based on a reduced-complexity Least-Squares (LS) formulation to determine the compensated transform in the final processing stage. The proposed approach is compared to the previous (range-dependent matched filter) compensated transform using experimental measurements, where a 5 dB signal-to-interference-plus-noise (SINR) improvement is demonstrated.

Index Terms—FMCW, stretch processing, dual-function radar/communications, range sidelobe modulation

I. INTRODUCTION

The explosion of wireless communications, for both military and commercial applications, along with enduring wideband requirements for radar sensing has created an ever-worsening congestion of RF spectrum [1]. This spectrum congestion has spurred two separate but complementary branches of research, namely dynamic spectral access (DSA) and co-design, to improve the efficacy of spectral usage by a multitude of users and functions. With DSA multiple users strive to coexist within the same band with minimal interference to one another (e.g. [2], [3]), whereas with co-design multiple RF functions are performed concurrently by the same system (e.g. radar and communications) to more efficiently use a particular frequency band (e.g. [4]–[14]).

The recently proposed phase-attached radar-communications (PARC) approach combines radar and communication functions through the summation of their separate continuous phase structures, with the resulting FM waveform being amenable to high-power transmitters that are common for radar applications [9], [15]. Specifically, the PARC formulation involves the phase addition of a baseline FM radar waveform with a communication signal implemented via continuous phase modulation (CPM)

[16]. Consequently, both power and spectral efficiency are maintained.

The pulsed PARC framework [9], [17] was recently extended to an FM continuous wave (FMCW) implementation referred to as FMCW PARC [13]. The use of a recent compensated form of stretch processing [18] then permits the use of large transmit bandwidths to achieve fine radar range resolution as well as relatively high communication data rates. This variant of stretch processing involves replacing the final fast Fourier transform (FFT) stage with a compensation transform that can be viewed as a range-dependent matched filter bank.

The unique communication data in each sweep of FMCW PARC realizes a waveform-agile transmission mode in which the emitted waveform changes from sweep to sweep. Consequently, the clutter incurs a range sidelobe modulation (RSM) effect [6], [9], [15] that hinders effective cancellation and takes the form of smearing across Doppler. While the compensated stretch processing does correct for the SNR loss that occurs due to deviation of the emitted waveform from the reference signal, it does not address this RSM degradation.

Here, a Least-Squares based compensation transform is proposed that is essentially a range-dependent mismatched filter (MMF) bank. The objective with this type of mismatched filtering is to better homogenize the filter responses—despite the sweep-to-sweep changing waveform structure—by forcing a common desired response across all sweeps of the CPI [19], [20]. The optimal solution to forcing a particular desired solution is shown to be rather computationally costly, which motivates development of the reduced-complexity approach presented here.

II. FMCW PARC

In [13] the passband FMCW PARC waveform was defined as

$$s(t; \mathbf{x}) = \cos(\psi_r(t) + \psi_c(t; \mathbf{x})) \quad (1)$$

where $\psi_r(t)$ is the (passband) radar phase component and $\psi_c(t; \mathbf{x})$ is the communication phase component, both of which are continuous. The communication phase is obtained by modulating the M -ary symbol sequence $\mathbf{x} = [x_0 x_1 x_2 \dots]$ with CPM, where $x_n \in \{\pm 1, \pm 3, \dots, \pm(M-1)\}$ and $m = \log_2 M$ is the number of bits per symbol. The radar phase is the integral of the radar instantaneous frequency $f_r(t)$ as

$$\psi_r(t) = 2\pi \int_0^t f_r(\tau) d\tau. \quad (2)$$

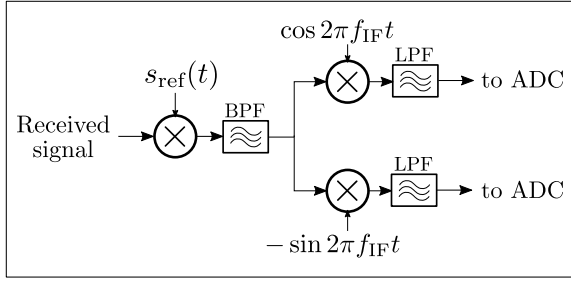


Fig. 1. Stretch processing using reference signal $s_{\text{ref}}(t)$ and intermediate frequency stage.

Here, $f_r(t)$ follows a down-chirped sawtooth wave. For the i th sweep of duration T_{sw} the instantaneous frequency is therefore defined as

$$f_r(iT_{\text{sw}} \leq t < (i+1)T_{\text{sw}}) = f_0 - \gamma(t - iT_{\text{sw}}), \quad (3)$$

where f_0 is the starting (passband) frequency and $\gamma = B/T_{\text{sw}}$ is the chirp rate for swept bandwidth B .

The communication phase component during the i th sweep, i.e. $iT_{\text{sw}} \leq t < (i+1)T_{\text{sw}}$, is [9], [13], [16]

$$\psi_c(t; \mathbf{x}) = \pi h \int_0^t \sum_{n=0}^{(i+1)N_c-1} x_n g(\tau - nT_c) d\tau, \quad (4)$$

where T_c is the symbol interval, $N_c = \frac{T_{\text{sw}}}{T_c}$ is the number of communication symbols per sweep, h (a rational number) is the CPM modulation index, and $g(t)$ is the (unit area) CPM shaping filter. The communication symbol rate is thus $B_c = \frac{1}{T_c}$ symbols/s, and the data rate is mB_c bits/s. The CPM parameters h , T_c , $g(t)$ and M uniquely specify the spectrum of the communication signal component and hence the receiver bandwidth for a given range profile.

The modulation index h is a very important system parameter from a radar performance perspective as it controls the degree of similarity across the sweep-to-sweep changing radar/communication waveforms. It was shown experimentally for FMCW PARC in [13] that greater similarity translates to enhanced coherence across the clutter return samples of different sweeps in the CPI, and consequently reduced RSM.

III. OPTIMIZING STRETCH PROCESSING COMPENSATION FOR FMCW PARC

The analog portion of the stretch processing system model (Fig. 1) consists of mixing the received signal with a reference $s_{\text{ref}}(t)$ down to intermediate frequency (IF) f_{IF} , which is subsequently bandpass filtered (BPF), further mixed down to baseband, and then lowpass filtered (LPF). Given an IF bandwidth B_{IF} and chirp rate γ , the range swath that can be observed after stretch processing is

$$\Delta r = \frac{cB_{\text{IF}}}{2\gamma} = r_{\text{far}} - r_{\text{near}}, \quad (5)$$

for c the speed of light, and with r_{near} and r_{far} the near and far edges of the range swath, respectively. This range swath likewise corresponds to the band of IF frequencies $[f_{\text{IF}} - \frac{B_{\text{IF}}}{2}, f_{\text{IF}} + \frac{B_{\text{IF}}}{2}]$.

The reference signal $s_{\text{ref}}(t)$ is designed to be a time and frequency shifted version of $\cos(\psi_r(t))$ that depends only on the radar phase component. For alignment range r_a (where $r_{\text{near}} \leq r_a \leq r_{\text{far}}$), the reference signal is thus

$$s_{\text{ref}}(t) = \cos\left(2\pi f_a \cdot \left(t - \frac{2r_a}{c}\right) + \psi_r\left(t - \frac{2r_a}{c}\right)\right), \quad (6)$$

where

$$f_a = f_{\text{IF}} - \frac{B_{\text{IF}}}{2} + \frac{r_a - r_{\text{near}}}{r_{\text{far}} - r_{\text{near}}} B_{\text{IF}} \quad (7)$$

is the IF frequency corresponding to range r_a .

Because of the additional communication component in (1), the response after mixing/filtering via Fig. 1 does not have a tonal structure that could be fully compressed via FFT like standard stretch processing. However, it was shown in [18] that full SNR gain can be achieved through the use of a compensated transform that accounts for deviations from the reference signal.

The complex baseband received signal during the i th sweep of a CPI can be expressed as

$$y_i(t; \mathbf{x}_i) = \Phi_{\text{LPF}}\left\{\Phi_{\text{BPF}}\left\{s_{\text{ref}}(t)\tilde{y}_i(t; \mathbf{x}_i)\right\}\exp(-j2\pi f_{\text{IF}}t)\right\} \quad (8)$$

where $\mathbf{x}_i = [x_0, \dots, x_{(i+1)N_c-1}]$ is the associated symbol sequence, $\Phi_{\text{BPF}}\{\bullet\}$ and $\Phi_{\text{LPF}}\{\bullet\}$ represent the bandpass and lowpass filtering operations from Fig. 1, respectively, and

$$\tilde{y}_i(t; \mathbf{x}_i) = s_i(t; \mathbf{x}_i) * z_i(t) + u_i(t) \quad (9)$$

is the signal captured at the receive antenna. Here $s_i(t; \mathbf{x}_i)$ is the waveform transmitted during the i th sweep, $z_i(t)$ represents the scattering from the environment, and $u_i(t)$ is the noise process. The complex baseband received signal of (8) is then sampled to obtain the vector

$$\mathbf{y}_i(\mathbf{x}_i) = [y_i(\tau_a; \mathbf{x}_i), \dots, y_i(\tau_a + (L-1)T_s; \mathbf{x}_i)]^T, \quad (10)$$

where $\tau_a = \frac{2r_a}{c}$ and L is the number of received samples per sweep obtained by I/Q sampling the mixer output at f_s samples/s, which corresponds to sampling period $T_s = 1/f_s$. The sampling rate satisfies $f_s > B_{\text{IF}}$ for sufficient fidelity, and is chosen such that $L = T_{\text{sw}}/T_s$ is an integer.

For a normalized point scatterer at range r during the i th sweep, the signal response (in the absence of noise) prior to sampling can be expressed as

$$p_i(t, r; \mathbf{x}_i) = \Phi_{\text{LPF}}\left\{\Phi_{\text{BPF}}\left\{s_{\text{ref}}(t)s\left(t - \frac{2r}{c}; \mathbf{x}_i\right)\right\}\exp(-j2\pi f_{\text{IF}}t)\right\}. \quad (11)$$

Sampling this point response therefore yields the vector

$$\mathbf{p}_i(r; \mathbf{x}_i) = [p_i(\tau_a, r; \mathbf{x}_i), \dots, p_i(\tau_a + (L-1)T_s, r; \mathbf{x}_i)]^T. \quad (12)$$

Thus, the range-dependent matched filter for range r is

$$\mathbf{w}_i(r; \mathbf{x}_i) = \frac{\mathbf{p}_i(r; \mathbf{x}_i)}{\|\mathbf{p}_i(r; \mathbf{x}_i)\|_2}, \quad (13)$$

which even for fixed r changes from sweep to sweep according to the communication sequence \mathbf{x}_i . The set of range-dependent matched filters in the i th sweep can be collected into the compensation matrix [18]

$$\mathbf{W}_i(\mathbf{x}_i) = [\mathbf{w}_i(r_{\text{near}}; \mathbf{x}_i) \cdots \mathbf{w}_i(r_{\text{near}} + (K-1)\delta r; \mathbf{x}_i)], \quad (14)$$

where K is the number of samples in the range profile, and δr is the range spacing, which is chosen smaller than the range resolution (i.e. $\frac{c}{2B}$), such that $r_{\text{far}} = r_{\text{near}} + (K - 1)\delta r$. It follows that the range profile estimate in the i th sweep is obtained by the matrix product

$$\widehat{\mathbf{z}}_i = \mathbf{W}_i^H(\mathbf{x}_i) \mathbf{y}_i(\mathbf{x}_i). \quad (15)$$

It is important to note that the filter bank $\mathbf{W}_i(\mathbf{x}_i)$ changes from sweep to sweep as the radar/communication waveform changes.

A discretized representation of normalized scatterer responses over the ranges of interest can be formed by collecting (12) for these discretized ranges into the matrix

$$\mathbf{P}_i(\mathbf{x}_i) = [\mathbf{p}_i(r_{\text{near}}; \mathbf{x}_i) \cdots \mathbf{p}_i(r_{\text{near}} + (K - 1)\delta r; \mathbf{x}_i)]. \quad (16)$$

Thus, application of the compensation transform of (14) yields the $K \times K$ matrix

$$\mathbf{D}_i(\mathbf{x}_i) = \mathbf{W}_i^H(\mathbf{x}_i) \mathbf{P}_i(\mathbf{x}_i), \quad (17)$$

which captures the mainlobe and sidelobe structure for each of these range-dependent matched filters. The mainlobe peak lies on the main diagonal of $\mathbf{D}_i(\mathbf{x}_i)$ and remains constant from sweep to sweep. Beyond the super/sub-diagonals close to the main diagonal that represent the mainlobe roll-off, the values of $\mathbf{D}_i(\mathbf{x}_i)$ vary from sweep to sweep due to the changing structure of the PARC FMCW waveform. This range sidelobe modulation (RSM) effect, when imposed upon the clutter, incurs a loss of coherence that limits the efficacy of clutter cancellation.

To combat RSM within this FMCW context, we seek to optimize the compensation matrix to limit the sweep-to-sweep changes in the correlation response such that the desired output approximates

$$\mathbf{W}_i^H(\mathbf{x}_i) \mathbf{P}_i(\mathbf{x}_i) \approx \mathbf{D}_{\text{dsr}}, \quad (18)$$

for some constant *desired* response \mathbf{D}_{dsr} . Determination of this *mismatched filter* (MMF) compensation transform can thus be formulated as the optimization problem

$$\mathbf{W}_{\text{MMF},i} = \arg \min_{\mathbf{W}} \|\mathbf{W}^H \mathbf{P}_i(\mathbf{x}_i) - \mathbf{D}_{\text{dsr}}\|_F^2, \quad (19)$$

where $\|\bullet\|_F^2$ is the squared Frobenius norm. A good choice for \mathbf{D}_{dsr} is the collection of responses for a FMCW waveform without the communication component, in which case

$$\mathbf{D}_{\text{dsr}} = \mathbf{A} \mathbf{P}_{\text{LFM}}, \quad (20)$$

where \mathbf{A} is the unitary DFT matrix, i.e. $\mathbf{A}^H \mathbf{A} = \mathbf{I}$, and \mathbf{P}_{LFM} is the matrix of responses from (16) when $s(t)$ is simply a down-chirped sawtooth LFM.

Unfortunately, direct computation of $\mathbf{W}_{\text{MMF},i}$ via (19) requires inverting the $L \times L$ matrix $\mathbf{P}_i(\mathbf{x}_i) \mathbf{P}_i^H(\mathbf{x}_i)$ for each sweep, which can be very large (for the experimental results here it is 25000×25000). Consequently, a reduced complexity approach is in order.

Instead of directly computing the entire MMF compensation transform, where each column is a range-dependent

mismatched filter, we take a two-step procedure that involves first determining the particular MMF for the alignment range, denoted as $\mathbf{w}_{\text{MMF},i}(r_a)$. Then by using the (approximate) time and frequency shifted structure of $\mathbf{P}_i(\mathbf{x}_i)$, all other range-dependent mismatched filters are obtained by time-shifting $\mathbf{w}_{\text{MMF},i}(r_a)$ and multiplying by the discrete-time complex sinusoid corresponding to the relative range difference between the range of interest r and alignment range r_a .

Because $\mathbf{w}_{\text{MMF},i}(r_a)$ is a discrete sequence, time-shifting (and frequency-shifting) the filter will result in aliasing of the time (and frequency) envelope(s). It is necessary to first estimate a continuous-time version of $\mathbf{w}_{\text{MMF},i}(r_a)$ (denoted $w_{\text{MMF},i}(t; r_a)$) before time and frequency shifting the filter, where $w_{\text{MMF},i}(\ell T_s; r_a) = \mathbf{w}_{\text{MMF},i}(r_a)$ for $\ell = 0, 1, \dots, L - 1$. Once determined, the i th filter corresponding to range $r = r_{\text{near}} + k\delta r$ for $k = 0, 1, \dots, K - 1$ is

$$w_{\text{MMF},i}(t; r_{\text{near}} + k\delta r) = w_{\text{MMF},i}(t - \tau_k; r_a) e^{j2\pi\gamma\tau_k(t - \tau_k)}, \quad (21)$$

where

$$\tau_k = \frac{2(r_{\text{near}} + k\delta r - r_a)}{c} \quad (22)$$

is the relative delay between the backscatter from range $r_{\text{near}} + k\delta r$ and the alignment range r_a . Finally, $\mathbf{w}_{\text{MMF},i}(r_{\text{near}} + k\delta r)$ is found by simply sampling (21) at $w_{\text{MMF},i}(\ell T_s; r_{\text{near}} + k\delta r)$ for $\ell = 0, 1, \dots, L - 1$.

Determination of $\mathbf{w}_{\text{MMF},i}(r_a)$ could be achieved by solving

$$\mathbf{w}_{\text{MMF},i}(r_a) = \arg \min_{\mathbf{w}} \|\mathbf{w}^H \mathbf{P}_i(\mathbf{x}_i) - \mathbf{d}_{\text{dsr}}(r_a)\|_2^2, \quad (23)$$

where $\mathbf{d}_{\text{dsr}}(r_a)$ is the row of \mathbf{D}_{dsr} associated with $\mathbf{w}_{\text{MMF},i}(r_a)$ in (18). However, this approach still requires inversion of the large $\mathbf{P}_i(\mathbf{x}_i) \mathbf{P}_i^H(\mathbf{x}_i)$ matrix. Instead, we *compress* $\mathbf{P}_i(\mathbf{x}_i)$ using the DFT via

$$\begin{aligned} \mathbf{P}_i^H(\mathbf{x}_i) \mathbf{w} &= \mathbf{P}_i^H(\mathbf{x}_i) \mathbf{A}^H \mathbf{A} \mathbf{w} \\ &= (\mathbf{A} \mathbf{P}_i(\mathbf{x}_i))^H \mathbf{A} \mathbf{w} \\ &= \mathbf{P}_{\text{F},i}^H(\mathbf{x}_i) \mathbf{w}_{\text{F}} \end{aligned} \quad (24)$$

where $\mathbf{P}_{\text{F},i}(\mathbf{x}_i) = \mathbf{A} \mathbf{P}_i(\mathbf{x}_i)$ and $\mathbf{w}_{\text{F}} = \mathbf{A} \mathbf{w}$ are the Fourier transforms of $\mathbf{P}_i(\mathbf{x}_i)$ and \mathbf{w} , respectively. Because a FMCW PARC waveform involves relatively small deviations from the baseline FMCW chirping structure, the transformed matrix $\mathbf{P}_{\text{F},i}(\mathbf{x}_i)$ has most of its energy within a band centered on the main diagonal, the width of which depends on the bandwidth of the communication signal component.

By exploiting this banded structure we can reduce the dimensionality of the matrix inverse by selecting a *submatrix* corresponding to alignment range r_a within the full matrix $\mathbf{P}_{\text{F},i}(\mathbf{x}_i)$. To illustrate, consider an example where the communication bandwidth is 15% of the IF bandwidth B_{IF} . Figure 2 shows the squared magnitude of $\mathbf{P}_{\text{F},i}(\mathbf{x}_i)$ (in dB) for this case. Note that for alignment range r_a , a majority of the energy is contained within the white box. Thus, we can extract the submatrix $\tilde{\mathbf{P}}_{\text{F},i}(\mathbf{x}_i; r_a)$ which has dimension $N \times M$ (for $N < L$ and $M < K$) to determine $\mathbf{w}_{\text{MMF},i}(r_a)$ with only a $N \times N$ matrix inversion (for the experimental results here $N = 500$ is used).

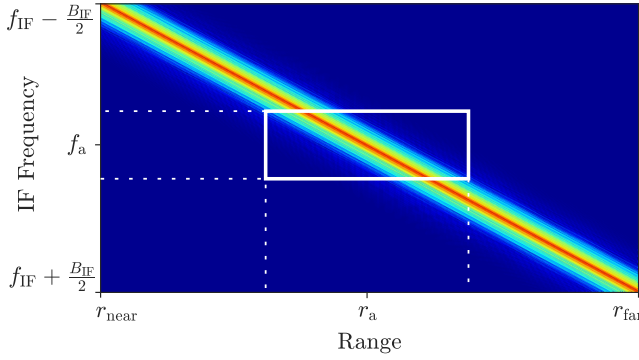


Fig. 2. Example of partially compressed matrix $|\mathbf{P}_{F,i}(\mathbf{x}_i)|^2$ (in dB) with submatrix $|\tilde{\mathbf{P}}_{F,i}(\mathbf{x}_i)|^2$ (in dB) outlined in white.

The submatrix $\tilde{\mathbf{P}}_{F,i}(\mathbf{x}_i; r_a)$ is related to $\mathbf{P}_{F,i}(\mathbf{x}_i)$ as

$$\tilde{\mathbf{P}}_{F,i}(\mathbf{x}_i; r_a) = \mathbf{U}^T \mathbf{P}_{F,i}(\mathbf{x}_i) \mathbf{V}, \quad (25)$$

where \mathbf{U} is an $L \times N$ matrix and \mathbf{V} is a $K \times M$ matrix. These selection matrices are constructed such that they precisely extract $\tilde{\mathbf{P}}_{F,i}(\mathbf{x}_i; r_a)$ (the white box in Fig. 2). Using this submatrix, (19) can therefore be approximated as

$$\tilde{\mathbf{w}}_{\text{MMF},i}(r_a) = \arg \min_{\mathbf{w}} \|\mathbf{w}^H \tilde{\mathbf{P}}_i(\mathbf{x}_i; r_a) - \tilde{\mathbf{d}}_{\text{dsr}}(r_a)\|_2^2, \quad (26)$$

where $\tilde{\mathbf{d}}_{\text{dsr}}(r_a) = \mathbf{d}_{\text{dsr}}(r_a) \mathbf{V}$ is the $1 \times M$ reduced dimension desired response and $\tilde{\mathbf{w}}_{\text{MMF},i}(r_a)$ is the $N \times 1$ reduced dimension MMF (in the frequency domain). Once obtained, $\tilde{\mathbf{w}}_{\text{MMF},i}(r_a)$ can be converted into the time-domain via

$$\mathbf{w}_{\text{MMF},i}(r_a) = \mathbf{A}^H \mathbf{U} \tilde{\mathbf{w}}_{\text{MMF},i}(r_a) \quad (27)$$

to form an optimized compensation transform that is still applied like (15).

IV. OPEN-AIR DATA COLLECTION AND RESULTS

Open-air measurements were collected using the FMCW PARC waveforms illuminating a traffic intersection in Lawrence, KS from the roof of Nichols Hall on the University of Kansas campus. Figure 3 shows the field of view and geometry for the experiment. Two S-band parabolic dish antennas with half-power beamwidth 12.3° (beamwidth shown in Fig. 3) were used to simultaneously transmit the FMCW PARC waveforms and receive the backscattered data. The transmitted waveforms and reference signals were generated using a Tektronix AWG70002A arbitrary waveform generator, and the backscattered echoes (after stretch mixing/filtering) were captured using a Rohde and Schwarz FSW 26 real-time spectrum analyzer.

The instantaneous frequency of the radar function $f_r(t)$ for the transmitted FMCW PARC waveforms follow a down-chirped sawtooth wave with starting and ending frequencies of 3.85 GHz and 3.35 GHz, respectively ($B = 500$ MHz bandwidth), for a $T_{\text{sw}} = 500 \mu\text{s}$ sweep time and $\gamma = 1$ MHz/ μs chirp rate. The intermediate frequency was set to $f_{\text{IF}} = 300$ MHz with $B_{\text{IF}} = 40$ MHz bandwidth (range swath of $\Delta r = 6000$ m). The near and far ranges were set to $r_{\text{near}} = 0$ m and $r_{\text{far}} = 6000$ m, respectively. The



Fig. 3. Field of view for FMCW PARC experimental demonstration for 12.3° transmit and receive antenna beamwidth.

TABLE I
FMCW STRETCH PROCESSING PARAMETERS

Description	Variable	Value
FMCW type	-	sawtooth
FMCW slope	-	down-chirp
Start frequency	f_0	3.85 GHz
Tx bandwidth	B	500 MHz
Sweep time	T_{sw}	500 μs
Chirp rate	γ	1 MHz/ μs
Intermediate freq.	f_{IF}	300 MHz
IF bandwidth	B_{IF}	40 MHz
Range swath	Δr	6000 m
Near range	r_{near}	0 m
Far range	r_{far}	6000 m
Alignment range	r_a	1050 m
Rx sampling rate	f_s	50 MHz
CPI	-	100 ms

alignment range was chosen as $r_a = 1050$ m ($f_a = 287$ MHz) which coincides with the middle of the intersection. The received data were sampled at 50 MHz after mixing/filtering. A total of 200 sweeps were captured to form a CPI having a total duration of 100 ms. The stretch processing parameters are shown in Table I. To facilitate a fair comparison, all test cases were transmitted back-to-back to illuminate approximately the same scene.

Figure 4 shows the radar-only baseline case while Figures 5 and 6 show the range-Doppler responses for FMCW PARC with a modulation index of $h = 1/8$ and 8 Mb/s data rate, for a total of 8×10^5 symbols transmitted in the 100 ms CPI. A raised-cosine shaping filter with duration $4T_c$ was used for $g(t)$ from (4). Figure 5 is generated using the (matched filter) compensation transform developed in [18] while Fig. 6 is obtained when the new MMF compensation transform is applied. In both cases the zero-Doppler clutter is suppressed using a simple projection, and a Hamming window is applied across the pulses to reduce Doppler sidelobes. While both cases do exhibit some RSM residue relative to the baseline case of Fig. 4, it is clear that the MMF approach (Fig. 6) substantially reduces this residue compared to the MF case (Fig. 5). Specifically, the average noise + residual clutter is approximately 5 dB lower in Fig. 6 than it is in Fig. 5, thus facilitating better target visibility. It is important to note that

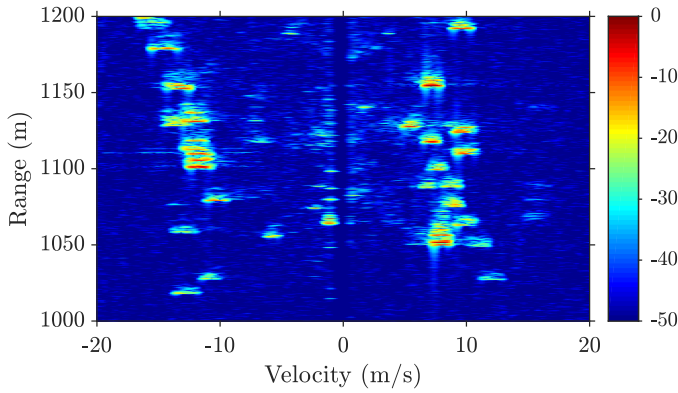


Fig. 4. Range-Doppler response for traditional stretch processed FMCW.

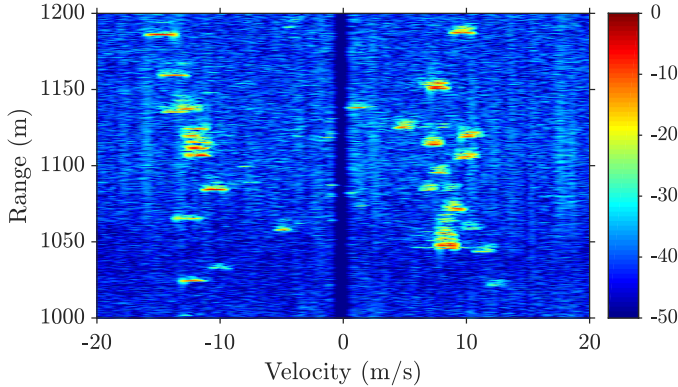


Fig. 5. Range-Doppler response for FMCW PARC with parameter values $h = 1/s$ and 8 Mb/s data rate obtained with the compensated transform (range-dependent matched filtering).

any kind of mismatched filtering enhances noise compared to matched filtering. This 5 dB improvement subsumes the reduction in SNR due to noise enhancement.

V. CONCLUSIONS

A pulsed version of PARC has previously been shown to be a feasible means with which to incorporate a data stream into a high-power radar emission. It was more recently demonstrated that an FMCW version can achieve even higher data rates due to the "always on" structure while simultaneously facilitating a wideband radar capability through the use of a compensated form of stretch processing on receive. Here this compensated stretch processing approach is modified within a reduced-complexity Least-Squares formulation to realize a sequence of mismatched filter banks that additionally compensate for the radar sidelobe modulation that is naturally incurred by altering the baseline radar waveform when incorporating a communication capability. It was shown using experimental measurements that residual clutter suppression of 5 dB can be obtained, thereby improving target visibility while maintaining a data rate on the order of several Mbps.

REFERENCES

[1] H. Griffiths, L. Cohen, S. Watts, E. Mokole, C. Baker, M. Wicks, and S. Blunt, "Radar spectrum engineering and management: technical and regulatory issues," *Proc. IEEE*, vol. 103, no. 1, Jan. 2015.

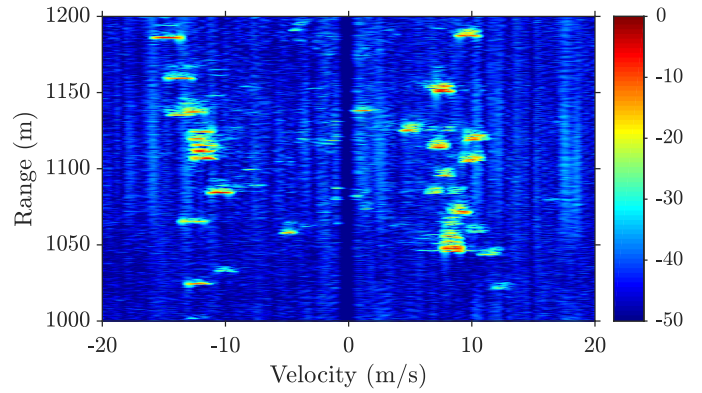


Fig. 6. Range-Doppler response for PARC parameter values $h = 1/s$ and 8 Mb/s data rate obtained with the MMF compensated transform.

[2] D.B. Rawat, M. Song, and S. Shetty, *Dynamic Spectrum Access for Wireless Networks*. Switzerland: Springer International Publishing, 2015.

[3] J.G. Metcalf, C. Sahin, S.D. Blunt, and M. Rangaswamy, "Analysis of symbol-design strategies for intrapulse radar-embedded communications," *IEEE Trans. Aerosp. Electron. Syst.*, vol. 51, no. 4, Oct. 2015.

[4] S.D. Blunt and E.S. Perrins, eds., *Radar & Communication Spectrum Sharing*. London, UK: IET, 2018.

[5] C. Sturm, T. Zwick, and W. Wiesbeck, "An OFDM system concept for joint radar and communications operations," *IEEE Vehicular Tech. Conf.*, Apr. 2009.

[6] S.D. Blunt, M.R. Cook, and J. Stiles, "Embedding information into radar emissions via waveform implementation," *Intl. Waveform Diversity and Design Conf.*, Aug. 2010.

[7] X. Chen, X. Wang, S. Xu, and J. Zhang, "A novel radar waveform compatible with communication," *Intl. Conf. on Comp. Problem-Solving*, Oct. 2011.

[8] M. Nowak, M. Wicks, Z. Zhang, and Z. Wu, "Co-designed radar-communication using linear frequency modulation waveform," *IEEE Aerosp. Electron. Syst. Mag.*, vol. 31, no. 10, Oct. 2016.

[9] C. Sahin, J. Jakobosky, P.M. McCormick, J.G. Metcalf, and S.D. Blunt, "A novel approach for embedding communication symbols into physical radar waveforms," *IEEE Radar Conf.*, May 2017.

[10] B. Ravenscroft, P.M. McCormick, S.D. Blunt, J. Jakobosky, and J.G. Metcalf, "Tandem-hopped OFDM communications in spectral gaps of FM noise radar," *IEEE Radar Conf.*, May 2017.

[11] P.M. McCormick, S.D. Blunt, and J.G. Metcalf, "Simultaneous radar and communications emission from a common aperture, part I: theory," *IEEE Radar Conf.*, May 2017.

[12] P.M. McCormick, C. Sahin, S.D. Blunt, and J.G. Metcalf, "Physical waveform optimization for multiple-beam multifunction digital arrays," *The Asilomar Conf. on Signals, Systems, and Computers*, Oct. 2018.

[13] —, "FMCW implementation of phase-attached radar-communications," *IEEE Radar Conf.*, Apr. 2019.

[14] C. Sahin, P.M. McCormick, J.G. Metcalf, and S.D. Blunt, "Power-efficient multi-beam phase-attached radar/communications," *IEEE Radar Conf.*, Apr. 2019.

[15] C. Sahin, J.G. Metcalf, and S.D. Blunt, "Characterization of range sidelobe modulation arising from radar-embedded communications," *Intl. Conf. on Radar Syst.*, Oct. 2017.

[16] J.B. Anderson, T. Aulin, and C.E. Sundberg, *Digital Phase Modulation*. New York, NY: Springer US Publishing, 1986.

[17] C. Sahin, J.G. Metcalf, A. Kordik, T. Kendo, and T. Corigliano, "Experimental validation of phase-attached radar/communications: Radar performance," *Intl. Conf. on Radar*, Aug. 2018.

[18] D.M. Hemmingsen, P.M. McCormick, S.D. Blunt, C. Allen, A. Martone, K. Sherbondy, and D. Wikner, "Waveform-diverse stretch processing," *IEEE Radar Conf.*, Apr. 2018.

[19] C. Sahin, J.G. Metcalf, and S.D. Blunt, "Filter design to address range sidelobe modulation in transmit-encoded radar-embedded communications," *IEEE Radar Conf.*, May 2017.

[20] L. Harnett, D. Hemmingsen, P.M. McCormick, S.D. Blunt, C. Allen, A. Martone, K. Sherbondy, and D. Wikner, "Optimal and adaptive mismatch filtering for stretch processing," *IEEE Radar Conf.*, Apr. 2018.